Dynamic Sorption and Transport of Water Vapor in Dense Polyimide Membranes

Chuyi Zeng,[1,2] Jiding Li,[1] Tianquan Chen,[1] Jian Chen,[1] Cuixian Chen[1]

[1]*Department of Chemical Engineering, Membrane Technology and Engineering Research Center, Tsinghua University, Beijing 100084, People's Republic of China*
[2]*The Research Center of the Ministry of Education for Chemical Engineering Process Simulation and Optimization, Xiangtan University, Hunan 411105, People's Republic of China*

Received 26 October 2005; accepted 11 January 2006
DOI 10.1002/app.24265
Published online in Wiley InterScience (www.interscience.wiley.com).

ABSTRACT: Series of polyimide membranes were synthesized using varied monomers such as pyromellitic dianhydride, 3,3′4,4′-benzophenonetetracarboxylic dianhydride, 4,4′-diaminodiphenylether, 4,4′-diaminodiphenylmethane, and phenylenediamine, and the properties of polyimide membranes were measured by experimental techniques. The dynamic sorption and transport processes of water vapor in those dense polyimide membranes were measured using computer on-line recorded gravimetric sorption method at 298.15 and 308.15 K. Modeling of these processes involved the total change of excess Gibbs free energy, which was considered as a sum of three parts calculated by the modified Scatchard-Hildebrand model, Flory-Huggins theory, and linear viscoelastic theory, respectively. The calculated results were in agreement with the experimental data and the maximal relative deviation was no more than 8.57% and the average relative deviation is 4.62%. The calculated results had also shown that this model describe not only Fickian diffusion but also non-Fickian very well. Furthermore, the influence of chemical structure, morphological structure, etc. of polyimide membranes on the water sorption concentration and water diffusion coefficient were interpreted by considering the experimental data and calculation results. J Appl Polym Sci 102: 2189–2198, 2006

Key words: membranes; calculations; polyimide; diffusion

INTRODUCTION

Polyimides are a class of thermally stable polymers that are often prepared from dianhydride and diamine monomers. They are usually prepared by the so-called two-step method in which a dianhydride and a diamine are allowed to undergo condensation polymerization to synthesize a poly(amic acid) (PAA) precursor and subsequently, and then the precursor is converted thermally or chemically to the final polyimide.[1,2] It is known that some polyimides have excellent thermostability, mechanical, electrical, and solvent-resistance properties. Moreover, some other polyimides show high selectivity in dehydration of alcohol at a wide range of water concentrations. Permeation of water vapor in polyimides is an extremely important factor for many practical applications. For electronic, composite, or adhesive applications of polyimides, polyimide use generally requires low permeation to water vapor, since sorbed water not only affects performance but also causes metal corrosions, failures of adhesion, and degradation of dielectric properties.[2–8] However, in the development of polyimides as vapor separation membranes, particularly for dehumidification of gases, air, and organic vapors, polyimide membranes with high water vapor permeability have attracted great interest. Consequently, in the development and selection of polyimide membrane for a predefined task, it is essential to understand the factors influencing water vapor permeability and selectivity as well as thermal and chemical properties of polymers. Furthermore, the water vapor may influence sorption and transport by inducing morphological changes to the polyimide membrane owing primarily to its hydrogen bonding nature and other polar interactions with the polymer.[9,10] Quantitative descriptions of the dynamics and thermodynamics of such phenomena are therefore essential for the design and operation of these processes. Modeling of these processes involves the solution of dynamic diffusion equation with associated boundary conditions. Penetrant transport in polymeric membrane often deviates from the Fickian law, and leads to anomalous or non-Fickian diffusion behavior. The diffusion mechanism is very complicated, usually associated with the rearrangement of the polymer structure to accommodate penetrant molecules. The diffusion of small penetrant

Correspondence to: J. Li (lijiding@mail.tsinghua.edu.cn).
Contract grant sponsor: National Natural Science Foundation; contract grant number: 20276034.
Contract grant sponsor: National Basic Research Program of China (973 Program); contract grant number: 2003CB615701.

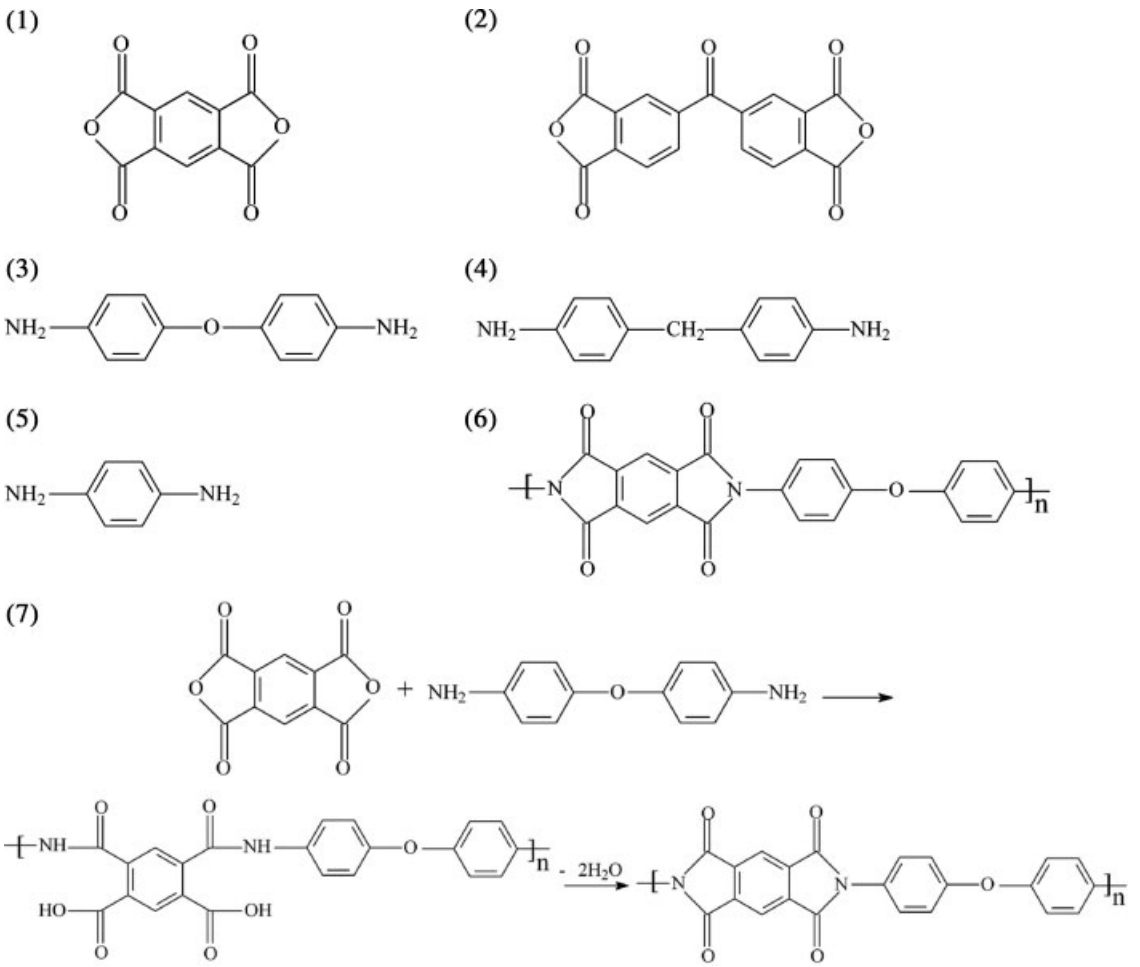

Scheme 1 The structures of polyimide monomers (1) PMDA; (2) BTDA; (3) ODA; (4) MDA; (5) PDA; (6) example of polyimide, PMDA-ODA; and (7) synthesis of PMDA-ODA polyimide by two-step method.

molecules into fully amorphous polymers has been divided into three basic mode of transport, depending on the relative rates of penetrant diffusion and polymer chain relaxation[11]: (1) Case I or Fickian diffusion occurs when the diffusion rate of penetrant molecules is much slower than the polymer chain relaxation; (2) Case II diffusion occurs when the penetrant diffusion rate is much faster than the polymer chain relaxation; and (3) Case III or non-Fickian diffusion occurs when the penetrant mobility and polymer chain relaxation rates are similar. To describe the mechanism of diffusion, especially for the sigmoid sorption curve, several models should be found from literature.[12,13] In our previous work, we have established a novel transport model to calculate well the dynamic transport behaviors of penetrant in polymeric membranes.[14]

In the present work, series of polyimide membrane materials have been synthesized using variable monomers, and the properties of polyimide membranes have been measured by experimental techniques.[1,15,16] We also present the results of water vapor dynamic sorption and transport behavior in the polyimides with different molecular structures measured by computer online recorded gravimetric sorption (GS) method. The model is used to calculate the diffusions of water vapor in five kinds of polyimide membrane materials synthesized using two dianhydrides with three diamines as the monomers.

EXPERIMENTAL

Materials

All chemicals were purchased from Acros Organics (Geel, Belgium) and Fluka Chemical (Milwaukee, WI, USA). Pyromellitic dianhydride (PMDA), 3,3′4,4′-benzophenonetetracarboxylic dianhydride (BTDA), 4,4′-diaminodiphenylether (ODA), 4,4′-diaminodiphenylmethane (MDA), and phenylenediamine (PDA) were purified before polymerization. *N*, *N*-dimethylformamide (DMF) was purified on distillation under reduced pressure over calcium hydride and stored over molecular sieves (4 Å).

All the monomers of polyimide are shown in Scheme 1, and the structure of PMDA-ODA, as an example of polyimide, is also shown therein.

TABLE I
The Physical Property Parameters of Polyimide Membranes

Polyimide	ρ (g cm^{-3})	l (μm)	T_g (K)	M[a] (g mol^{-1})	V_w (cm^3 mol^{-1})	FFV
PMDA-ODA	1.413	32.0	572	382.31	186.60	0.1034
PMDA-MDA	1.357	33.0	581	380.36	191.33	0.1126
BTDA-PDA	1.405	36.0	551	394.29	193.80	0.1024
BTDA-ODA	1.373	34.0	544	486.39	242.60	0.1097
BTDA-MDA	1.337	38.0	531	484.39	247.33	0.1125

[a] M, the molecular weight of the repeating units of polyimide polymers.

Preparation of polymeric membrane

First, diamine was added to the reaction vessel, and dissolved in DMF. Second, dianhydride was added to reach the solid concentration of about 12%, and then this solution was stirred under nitrogen atmosphere for 5 h at room temperature to prepare PAA.

The obtained PAA solution was cast on a glass plate to form a casting film with uniform thickness. Then the casting film was placed into a vacuum dryer for further heat treatment. The specimens produced were dried in vacuum for 2 days at 423.15 K to remove the solvent. The thicknesses of the obtained membranes were determined by using a micro screw gauge, and the results are listed in Table I.

Elemental analysis and IR spectrum

The elemental compositions of polyimide membranes were tested by EA 1112 Elemental Analyzer (Carlo Erba Instruments, Italy). The test results as well as the theoretical values for the proposed chemical structures of polymers were presented in Table II.

The polyimides were analyzed by Fourier transform infrared (FTIR) spectra, and were recorded on a Nicolet IR560 spectrometer. Spectra in the optical range of 400–4000 cm^{-1} were obtained by averaging 32 scans at a resolution of 4 cm^{-1}. The IR spectra of polyimide membranes are shown in Figure 1.

Effect of monomer structure on polyimide average spacing of chains

The powder X-ray diffraction patterns were recorded on a Bruker D8 diffractometer using 40 mA nickel-filtered CuK$_\alpha$ radiations ($\lambda = 1.5418$ Å) at a voltage of 40 kV with a step size of 0.02.

The average spacing values of polyimide chains (d-spacing) were obtained using the Bragg's diffraction equation ($2d \sin\theta = \lambda$).The results of the average spacing of polyimide chains are presented in Table III.

TABLE II
Elemental Compositions of Polyimide Obtained by Elemental Analysis[a]

	Elemental analysis (%)		
Polyimide	C	H	N
PMDA-ODA	67.30 (69.12)	2.50 (2.64)	7.32 (7.33)
PMDA-MDA	70.40 (71.05)	3.21 (3.18)	7.60 (7.37)
BTDA-PDA	69.63 (70.05)	2.64 (2.56)	7.25 (7.11)
BTDA-ODA	69.95 (71.60)	2.94 (2.90)	6.00 (5.76)
BTDA-MDA	72.13 (74.37)	3.38 (3.33)	5.80 (5.78)

[a] The data in brackets is theoretical value calculated from chemical structure.

Apparatus and procedure

Figure 2 shows the dynamic sorption apparatus. It contains the vapor generator, the data recorder, the vacuum system, and the thermostat.[17] The electrical balance (model BP211D, sensitivity 0.01 mg, made by Sartorius, Germany) is located in the thermostat. Prior to each sorption test, the membrane sample is put in the basket of the balance, and then the vacuum system is opened (pressure < 0.1 Pa) to desorb gas from the membrane over 8 h. Simultaneously, the temperature of the thermostat is regulated to a given value. Then the vapor is introduced into the balance compartment and the sorption test begins. The mass of the membrane is recorded by the data recorder in time until the sorption

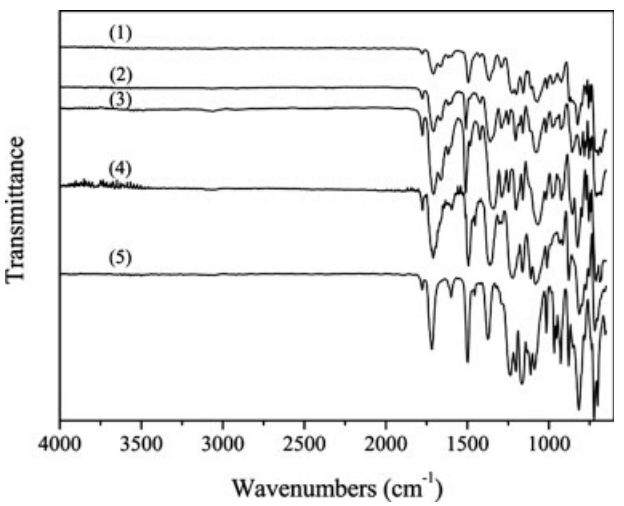

Figure 1 IR spectra of polyimide membranes: (1) BTDA-ODA; (2) BTDA-MDA; (3) BTDA-PDA; (4) PMDA-ODA; and (5) PMDA-MDA. (1) Vapor generator, (2) thermostat, (3) cushion jar, (4) centrifugal pump, (5) thermostat, (6) electrical banlance, (7) polymeric membrane, (8) thermometer, (9) balance compartment, (10) mercury barometer, (11) vacuum pump, and (12) data processer (V1-8, valves).

TABLE III
Average Spacing of Chains of Polyimide Membrane

Polyimide	2θ	*d*-spacing (Å)
PMDA-ODA	19.0	4.6
PMDA-MDA	18.0	4.9
BTDA-PDA	23.0	3.9
BTDA-ODA	20.5	4.3
BTDA-MDA	18.0	4.9

equilibrium, which is determined when no measurable change is observed within an hour, is obtained.

THEORY

It is considered that an infinite isotropy polymeric membrane with thickness l contacting with the vapor of penetrant. It is assumed that sorption equilibrium with penetrant of concentration m_1 is instantaneously established at the surface of polymeric membrane. Then, the diffusion of penetrant is conducted from the surface to the interior of membrane. The concentration of penetrant finally reaches equality in polymeric membrane. Sorption of penetrants in polymers is usually accompanied with a swelling in dimensions. This swelling gives rise to a stress. Consequently, polymer molecules begin to creep, and show a time- and place-dependent viscoelastic behavior, which also leads to a variation of membrane dimensions.

The mass conservation equation for transportation of penetrant in polymeric membrane is expressed as[18]:

$$J_1 = -\frac{D_0 C_1}{RT}\nabla\mu_1 \tag{1}$$

In the case of one dimension, eq. (1) is written as

$$\frac{\partial C_1}{\partial t} = \frac{\partial}{\partial x}\left(D_0 C_1 \frac{\partial \ln a_1}{\partial C_1}\frac{\partial C_1}{\partial x}\right) = \frac{\partial}{\partial x}\left(D_{12}\frac{\partial C_1}{\partial x}\right) \tag{2}$$

where

$$D_{12} = D_0 C_1 \frac{\partial \ln a_1}{\partial C_1} = D_0\left(1 + C_1\frac{\partial \ln \gamma_1}{\partial C_1}\right) \tag{3}$$

The activity coefficient of penetrant is expressed as follows:

$$\ln \gamma_1 = \left[\frac{\partial(G^{\mathrm{E}}/RT)}{\partial n_1}\right]_{T,P,n_2} \tag{4}$$

where the total change of excess Gibbs free energy of the sorption process is a sum of three parts

$$G^{\mathrm{E}} = U^{\mathrm{E}} + (pV)^{\mathrm{E}} - (TS)^{\mathrm{E}} \tag{5}$$

Consequently, the activity coefficient of solvent is calculated in terms of U^{E}, $(pV)^{\mathrm{E}}$, and $(TS)^{\mathrm{E}}$ parts:

$$\ln \gamma_1 = \ln \gamma_1^{U^{\mathrm{E}}} + \ln \gamma_1^{(pV)^{\mathrm{E}}} - \ln \gamma_1^{(TS)^{\mathrm{E}}} \tag{6}$$

For the U^{E} part, with the modified Scatchard-Hildebrand solution theory,[19] it is expressed as follows:

$$\ln \gamma_1^{U^{\mathrm{E}}} = \frac{v_1\phi_2^2}{RT}(1 - l_{12}) \times \left[(\sqrt{P}_1\delta_1 - \sqrt{P}_2\delta_2)^2 + (\sqrt{d}_1\delta_1 - \sqrt{d}_2\delta_2)^2\right] \tag{7}$$

For the $(pV)^{\mathrm{E}}$ part, according to the define of the excess property in thermodynamics, the $(pV)^{\mathrm{E}}$ is calculated as the following equation:

$$(pV)^{\mathrm{E}} = \Delta(pV) - \Delta(pV)^{\mathrm{id}} \tag{8}$$

The sorption is processed at a constant temperature and pressure, and the volume has no change in ideal mixing process in constant pressure. Thus, $\Delta(pV)^{\mathrm{id}}$ is equal to zero. To consider the effect of polymer creep influencing on the properties of membrane, the Voigt creep model of the linear viscoelastic solid is used in this work, and the constitutive equation[20] is written as

$$\varepsilon(t) = \frac{\sigma_0}{E}\left[1 - \exp\left(-\frac{tE}{\eta}\right)\right] \tag{9}$$

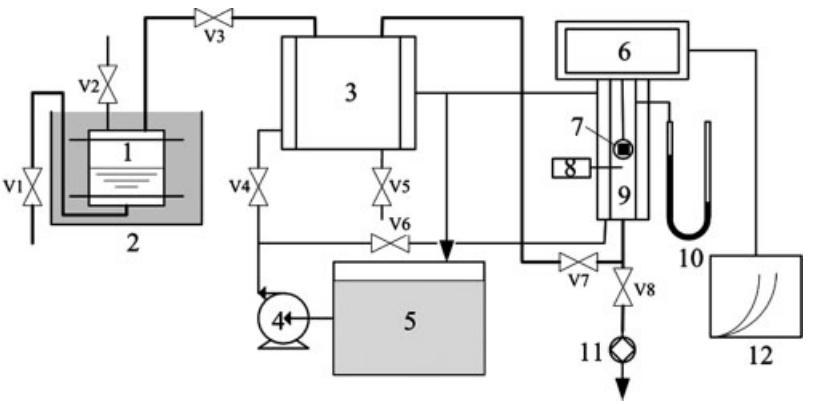

Figure 2 A schematic diagram of the apparatus used for measurement of the transport behavior.

TABLE IV
The Saturated Sorption Capacity of the Membranes and the Parameters (β, Γ, *P*, δ)

Polyimides	P[a]	δ ($J^{1/2}$ $cm^{-3/2}$)	m_{18} (g g^{-1}) 298.15 K	m_{18} (g g^{-1}) 308.15 K	β 298.15 K	β 308.15 K	Γ 298.15 K	Γ 308.15 K
PMDA-ODA	0.160	10.5	0.0230	0.0182	0.0326	0.0259	4.1153	3.9923
PMDA-MDA	0.205	10.1	0.0372	0.0250	0.0506	0.0338	3.9468	3.8277
BTDA-PDA	0.191	10.6	0.0143	0.0128	0.0201	0.0181	3.9075	3.7895
BTDA-ODA	0.149	10.1	0.0279	0.0249	0.0384	0.0344	4.2685	4.2158
BTDA-MDA	0.184	9.9	0.0345	0.0342	0.0327	0.0460	4.1048	4.0397

[a] Ref. 23.

It is assumed that the membranes are isotropic polymer, and so the strains are the same in three dimensionalities.

$$V = l_x(1+\varepsilon(\infty))l_y(1+\varepsilon(\infty))l_z(1+\varepsilon(\infty)) = V_0(1+\varepsilon(\infty))^3 \quad (10)$$

where V is the volume of sorbed penetrant together-with the membrane, and V_0 is the volume of dried membrane.

Moreover, the value of $\varepsilon(\infty)$ is very small, $(1+\varepsilon(\infty))^3 \ \ 1+3\varepsilon(\infty)$. Thus, it is expressed as

$$\varepsilon(\infty) = \frac{\sigma_0}{E} = \frac{V-V_0}{3V_0} = \frac{n_1 v_1}{3n_2 v_2} \quad (11)$$

Substituting eqs. (9) and (11) into eq. (8), and then substituting n_2v_2 by V_0 and leaving out the right hand side second term of eq. (8),

$$(pV)^{\mathrm{E}} = \Delta(pV) = P\Delta(V) = \sigma_0 V_0 \varepsilon(t) = En_2v_2\left(\frac{n_1v_1}{3n_2v_2}\right)^2\left[1-\exp\left(-\frac{tE}{\eta}\right)\right] \quad (12)$$

Thus, the $(pV)^{\mathrm{E}}$ part of penetrant activity coefficient is obtained as

$$\ln \gamma_1^{(pV)^{\mathrm{E}}} = \frac{2Ec_1v_1^2}{9RT}\left[1-\exp\left(-\frac{tE}{\eta}\right)\right] \quad (13)$$

where c_1 is defined as $n_1/(n_2v_2)$.

For the $(TS)^{\mathrm{E}}$ part, with Flory-Huggins equation[21] and the entropy change in an ideal binary volume mixing process[22]:

$$(TS)^{\mathrm{E}} = -RT\sum_i n_i \ln\frac{\phi_i}{x_i} = -RT\sum_i n_i \ln\frac{nv_i}{\sum_i n_i v_i} \quad (14)$$

Thus, considering $v_2 \gg v_1$, the $(TS)^{\mathrm{E}}$ part of penetrant activity coefficient is obtained as

$$\ln \gamma_1^{(TS)^{\mathrm{E}}} = \ln\left(\frac{v_1c_1}{1+v_1c_1}\right) - \frac{1}{1+v_1c_1} \quad (15)$$

Substituting eqs. (7), (13), and (15) into eq. (6), and then substituting $c_1 = \frac{m_1\rho_2}{M_1}$ and eq. (6) into eq. (3), we obtain

$$\frac{D_{12}}{D_0} = \left(1+\frac{v_1\rho_2m_1}{M_1}\right)^{-2} + \frac{2Ev_1^2\rho_2m_1}{9RTM_1}\left[1-\exp\left(-\frac{tE}{\eta}\right)\right] - \left[\frac{m_1v_1\rho_2}{M_1} - \left(\frac{m_1v_1\rho_2}{M_1}\right)^2\right] \times \left[\left(\sqrt{P_1}\delta_1 - \sqrt{P_2}\delta_2\right)^2 + \left(\sqrt{d_1}\delta_1 - \sqrt{d_2}\delta_2\right)^2\right]\frac{2v_1}{RT}(1-l_{12}) + 1 \quad (16)$$

As shown in eq. (16), the mutual diffusion coefficient of penetrant in polymeric membrane is time- and place-dependent.The dimensionless mass concentration, diffusion coefficient, distance, and time are defined as follows:

$$m = \frac{m_1}{m_{1\infty}}, \quad D = \frac{D_{12}}{D_0}, \quad \xi = \frac{2x}{l}, \quad \tau = \frac{4tD_0}{l^2}$$

Thus, eqs. (2) and (16) are written as dimensionless form. The transport equation, initial and boundary condition are written as

$$\frac{\partial m}{\partial \tau} = \frac{\partial}{\partial \xi}\left(D(m)\frac{\partial m}{\partial \xi}\right) \quad (17)$$

$$D(m) = (1+m\beta)^{-2} + \alpha m\left[1-\exp\left(-\frac{\tau}{Q}\right)\right] + 1 - \Gamma(1-l_{12})[m\beta-(m\beta)^2] \quad (18)$$

$$\tau = 0, \quad -1 \leqslant \xi \leqslant 1, \quad m = 0$$

$$\tau > 0, \quad \xi = \pm 1, \quad m = 1$$

TABLE V
The Optimal Model Parameters

	α	Q	l_{12}
PMDA-ODA	10.3145	0.0166	−1.534
PMDA-MDA	63.7159	0.0175	−2.164
BTDA-PDA	62.1005	0.0011	7.798
BTDA-ODA	72.4915	0.0012	7.893
BTDA-MDA	66.2355	0.0005	6.841

where

$$\alpha=\frac{2E\nu_1\beta}{9RT},\ \beta=\frac{\nu_1\rho_2 m_{1\infty}}{M_1},\ Q=\frac{4D_0\eta}{l^2E},$$

and

$$\Gamma=\frac{2\nu_1}{RT}\left[\left(\sqrt{P_1}\delta_1-\sqrt{P_2}\delta_2\right)^2+\left(\sqrt{d_1}\delta_1-\sqrt{d_2}\delta_2\right)^2\right]$$

RESULTS AND DISCUSSIONS

The physical property parameters of polyimide membranes are presented in Table I, where free volume is calculated by Bondi's model of group contribution. As can be seen in Table I, with the same dianhydride the free volume values of polyimide membranes increase in the following order: PDA < ODA < MDA. It means that the free volume increases with the decreasing of density, and the higher the density, the lower the free volume is. The introduction of bridging atoms into diamines also contributes to the increase of free volume. With the same diamines, the free volume values of BTDA polyimides are larger than that of PMDA polyimides.

The test results of elemental compositions are in agreement with the theoretical values for the proposed chemical structure of polyimide membranes as presented in Table II. In addition, as shown in Figure 1, polyimide membranes showed representative imide carbonyl peaks, but no distinct amide groups, and this indicated that the polyimides had been fully imidized.

As shown in Table III, it is clear that with the same dianhydrides, the average spacings of polyimide chains decrease in the following order: PDA > ODA > MDA, which agrees with the order of density.

The dynamic sorption processes of water vapor in dense polyimide membranes at 298.15 and 308.15 K have been measured using computer on-line recorded GS method.

The model has some parameters, i.e., α, β, Γ, l_{12}, and Q, etc. β was given by multiplying the density of the polymer, the molar volume, and the balance sorption capacity of the vapor molecule, and then dividing the vapor molar molecular weight; Γ was a function of sys-

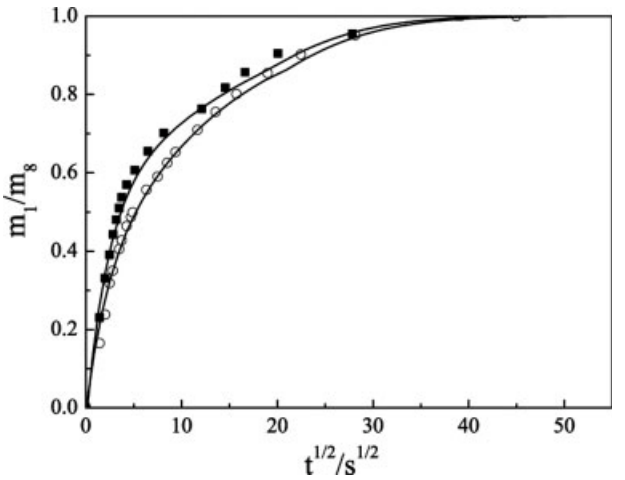

Figure 4 The comparison between calculated curves (solid lines) and experimental data (scatter points: ○, 298.15 K; ■, 308.15 K) of sorption process of water vapor in PMDA-MDA membrane.

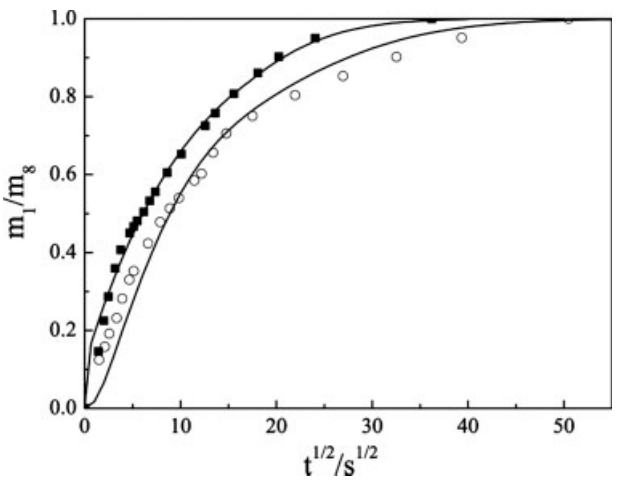

Figure 3 The comparison between calculated curves (solid lines) and experimental data (scatter points: ○, 298.15 K; ■, 308.15 K) of sorption process of water vapor in PMDA-ODA membrane.

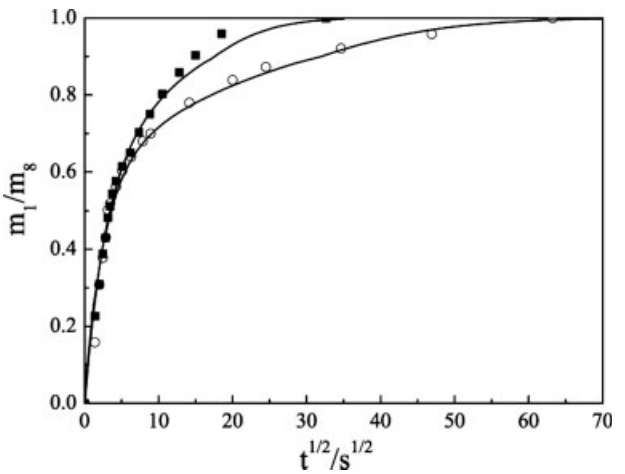

Figure 5 The comparison between calculated curves (solid lines) and experimental data (scatter points: ○, 298.15 K; ■, 308.15 K) of sorption process of water vapor in BTDA-PDA membrane.

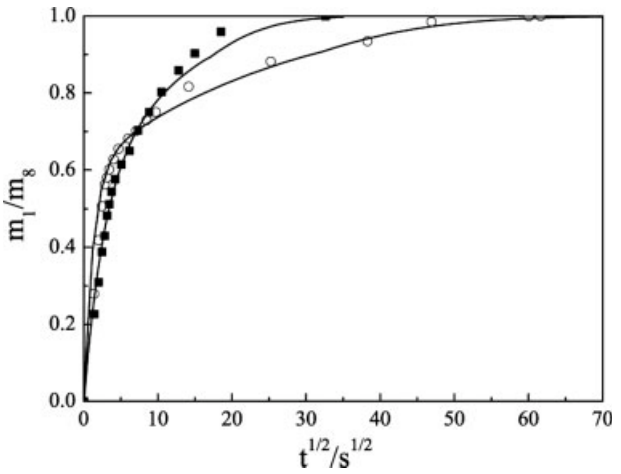

Figure 6 The comparison between calculated curves (solid lines) and experimental data (scatter points: ○, 298.15 K; ■, 308.15 K) of sorption process of water vapor in BTDA-ODA membrane.

tem temperature, and solubility parameters calculated by group-contribution method,[23] and molar volume of vapor molecule. The values of β and Γ are presented in Table IV. The parameters l_{12}, Q, and α are optimized by sorption experimental data. In this work, the partial differential equation [eq. (18)] is solved by implicit finite difference method of Crank-Nicolson form. Furthermore, the model parameters are optimized by simplex algorithm. In this way, the dynamic sorption curves of water vapor in dense polyimide membranes are calculated at 298.15 and 308.15 K.

The saturated mass concentrations of water in polyimide membranes, i.e. $m_{1\infty}$, can be interpreted by considering the major contributory factor of chemical affinity to water at the same temperature. Regarding chemical backbones, the chemical affinity of dianhydride monomeric segmers to water is in the increasing order: PMDA < BTDA. BTDA is more hydrophilic than PMDA. Accordingly, as shown in Table IV, $m_{1\infty}$ in PMDA polyimide membranes is greater than in BTDA polyimide membranes with the same diamine segmers. However for diamine segmers, it is in the increasing order: PDA < ODA < MDA, which agrees with the order of the values of $m_{1\infty}$ in polyimide membranes with the same dianhydrides segmers.

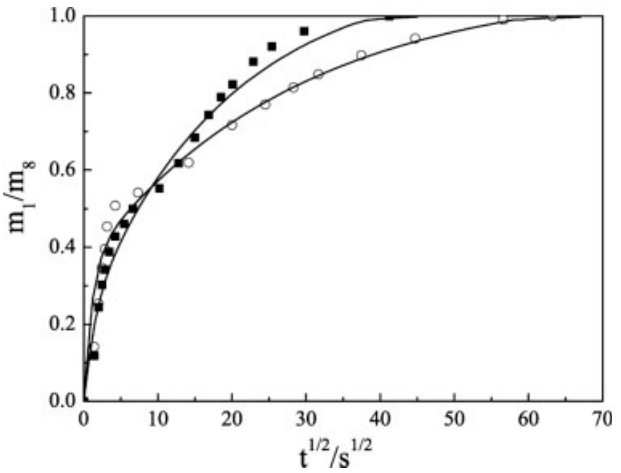

Figure 7 The comparison between calculated curves (solid lines) and experimental data (scatter points: ○, 298.15 K; ■, 308.15 K) of sorption process of water vapor in BTDA-MDA membrane.

Figures 3–7 show experimental data and calculation results of the sorption isotherms for water vapor in dense polyimide membranes at 298.15 and 308.15 K, which are dimensionless plots for m_1/m_∞ versus $t^{1/2}$. All the water sorption isotherms are reasonably well fitted by the model. The parameters α, Q, and l_{12} are derived from experimental data by calculations, which are summarized in Table V.

For the PMDA polyimide membranes, as shown in Figures 3 and 4, it is indicated that the sorption time decreases with temperature increasing in the whole sorption process. This is related to the higher diffusion velocity at higher temperature, which is in accordance with that expected in terms of the model. But for the BTDA polyimide membranes, as shown in Figures 5–7, the relationships between the sorption time and the temperature are more complicated. The m_1/m_∞ is smaller at 308.15 K than 298.15 K during the initial stage of water sorption in the BTDA polyimide membranes. The irregular phenomena of diffusion are also observed, as shown in Figures 5–7. This is probably because BTDA polyimide membranes have their bridging atoms as shown in Scheme 1, which increases the distance of benzene rings and enhances the chain flexibility. The interaction between small molecule and polymer strongly affects the diffusion characteristics.

Alfrey et al. have proposed a classification according to Fickian (Case I) and non-Fickian (Case II and anomalous) diffusions.[11] The amount of solvent absorbed per unit mass of polymer at time t, m_1, is represented by

$$m_1 = kt^N \tag{19}$$

where k is a constant and N is a parameter related to the diffusion mechanism, the value of which lies between 0.5 and 1. Equation (19) can be used to

TABLE VI
The Slope Parameters for Fitting Line of $\ln(m_t/m_\infty)$ vs $\ln t$

	T (K)	
	298.15	308.15
PMDA-ODA	0.50	0.485
PMDA-MDA	0.51	0.483
BTDA-PDA	0.70	0.649
BTDA-ODA	0.55	0.52
BTDA-MDA	0.51	0.48

describe solvent diffusional behaviors for any polymer + penetrant system whatever may be the temperature and the penetrant activity.

For Fickian (Case I) diffusion, $N = 0.5$; for Case II diffusion, $N = 1$; and for anomalous diffusion, $0.5 < N < 1$ in eq. (19).[24] N in eq. (19) is obtained from the linear plot of $\ln(m_1/m_\infty)$ with $\ln t$ in the initial stage of sorption isotherms. For the systems mentioned in this work, the slope parameters, N, is presented in Table VI. Figures 8 and 9 give some typical lines of $\ln(m_1/m_\infty)$ with $\ln t$ for water vapor's diffusion in polyimide membranes.

As presented in Table VI, the values of N for the sorption of water vapor in PMDA-ODA, PMDA-MDA, BTDA-ODA, and BTDA-MDA membranes are all about 0.5. It suggests that those sorption processes have representative characteristics of Fickian diffusion behavior according to Alfrey et al.'s theory. Moreover, for the sorption of water vapor in BTDA-PDA membrane at 298.15 and 308.15 K, the values of the slope parameter, N, are greater than 0.5 as presented in Table VI. Accordingly, the corresponding diffusion behavior transforms into typical non-Fickian diffusion.

The infinite dilute diffusion coefficients of water in polyimide membranes are calculated from the dimensionless time, as $\tau = (4tD_0)/l^2$. The results are listed in Table VII.

As shown in Table VII, the infinite dilute diffusion coefficients of water increase along with the temperature increasing in all systems, and the temperature dependence is well predicted by the model.

The coefficients of water diffusion vary in the range of 1.566×10^{15} to 8.652×10^{15} m^2 s^{-1}, and increased in the order: PMDA-ODA < PMDA-MDA < BTDA-PDA < BTDA-ODA < BTDA-MDA. These water diffusion coefficients in polyimide membranes can be interpreted by considering the major contributory factors of morphological structure at the same operation temperature. The glass transition temperatures of PMDA polyimide membranes are higher than BTDA because of the benzene ring without bridging atom, while the glass transition temperatures of BTDA polyimide membranes are lower due to their bridging atoms that increase the distance of benzene rings and enhance the chain flexibility. Accordingly, water molecule diffuses more rapidly in BTDA polyimide membranes than in PMDA polyimide membranes with the same diamine segmers.

However for diamine segmers, the order of the average spacings of polyimide chains is in the increasing order: PDA < ODA < MDA as presented in Table III, which agrees with the order of the free volume of their corresponding polyimides with the same dianhydride segmers. The diffusion coefficients of water in polyimide membranes at the same temperature increase in the order: BTDA-PDA < BTDA-ODA < BTDA-MDA and PMDA-ODA < PMDA-MDA, which is in accordance with that expected in terms of the free volume theory.

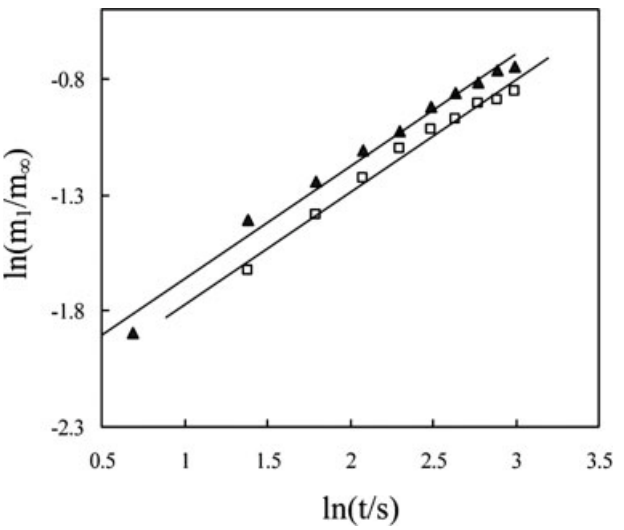

Figure 8 Relationships between the logarithm dimensionless mass, $\ln(m_t/m_\infty)$, and the logarithm time, $\ln t$, for water vapor in polyimide membrane (▲: PMDA-MDA; □: PMDA-ODA) at 308.15 K.

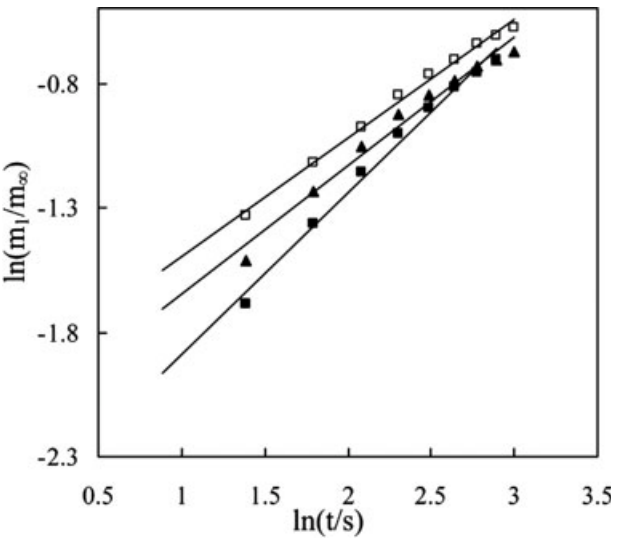

Figure 9 Relationships between the logarithm dimensionless mass, $\ln(m_t/m_\infty)$, and the logarithm time, $\ln t$, for ethanol vapor sorption in polyimide membrane (□: BTDA-MDA; ▲: BTDA-ODA; and ■: BTDA-PDA) at 308.15 K.

TABLE VII
The Infinite Dilute Diffusion Coefficients of Water in Polyimide Membranes

	D_0 (10^{15} m^2 s^{-1})	
	298.15 K	308.15 K
PMDA-ODA	1.566	1.983
PMDA-MDA	2.647	3.014
BTDA-MDA	5.498	8.652
BTDA-ODA	5.066	8.433
BTDA-PDA	4.688	7.922

TABLE VIII
The Average Relative Deviation between the Experimental Data and Calculation Results[a]

	Average relative deviation (%)	
	298.15	308.15
PMDA-ODA	4.62	5.79
PMDA-MDA	3.28	2.57
BTDA-PDA	8.57	2.43
BTDA-ODA	5.60	2.37
BTDA-MDA	8.12	2.80

[a] The average relative deviation is calculated as follows:

$$\frac{100\,\%}{n}\sum_1^n \mathrm{abs}((m_{\exp} - m_{cal})/m_{\exp}).$$

Table VIII presented the relative average deviation between the calculated results and experimental data for various data sets. The correlated and predicted results are in agreement with the experimental sorption curves of water in dense polyimide membranes. It is shown that this model is flexible and only a few model parameters are needed. As shown in Table VIII, the maximal relative deviation is 8.57% and the average relative deviation is 4.62% between the estimated results and experimental data.

CONCLUSIONS

Water vapor sorption and transport were investigated using a computer on-line recorded GS method for various dense polyimide membranes at 298.15 and 308.15 K. The sorption isotherms of water vapors in dense polyimide membranes were described successfully by model. According to Alfrey et al.'s theory, the sorption of water vapor in PMDA-ODA, PMDA-MDA, BTDA-ODA, and BTDA-MDA membranes had representative characteristics of Fickian diffusion behavior; as those for BTDA-PDA membrane, non-Fickian diffusion occurred therein. The coefficients of water diffusion in polyimide membranes varied in the range of 1.566×10^{15} to 8.652×10^{15} $m^2\ s^{-1}$, and increased in the order: PMDA-ODA < PMDA-MDA < BTDA-PDA < BTDA-ODA < BTDA-MDA.

NOMENCLATURE

a Activity (mol m^{-3})
c Concentration (mol m^{-3})
d Polarity parameter
D Diffusion coefficient ($m^2\ s^{-1}$)
E Young's modulus (Pa)
G Gibbs function (J mol^{-1})
J Flux (mol $m^{-2}\ s^{-1}$)
l Thickness of membrane [m]
M Molecular weight of repeating unit (g mol^{-1})
m Mass concentration (g g^{-1})
n Molar number
Q Dimensionless time for creep (s s^{-1})
p Pressure (Pa)
P Polarity parameter
R Gas constant (J $mol^{-1}\ K^{-1}$)
S Entropy (J $mol^{-1}\ K^{-1}$)
T Temperature (K)
t Time (s)
U Intrinsic energy (J mol^{-1})
v Molar volume ($m^3\ mol^{-1}$)
V Volume (m^3)
X Diffusion distance (m)

Greek letters

α, β, Γ Model parameters
γ Activity coefficient
δ Solubility parameter ($J^{1/2}\ cm^{-3/2}$)
ε Strain
μ_1 Chemical potential of penetrant (J mol^{-1})
η Viscosity (Pa s)
ρ Density (g m^{-3})
σ Stress (Pa)
τ Dimensionless time (s s^{-1})
ξ Dimensionless distance (m m^{-1})
ϕ Volume fraction ($m^3\ m^{-3}$)

Superscripts

E Excess property

Subscripts

1 Penetrant
2 Polymeric membrane
12 Mutual
c Creep
i Component i
0 Initial or dried state
∞ Equilibrium state

References

1. Wang, L.; Li, J.; Zhao, Z.; Chen, C. J Macromol Sci Pure Appl Chem 2006, A43, 305.
2. Seo, J.; Jeon, J.; Shui, Y. G.; Han H. J Polym Sci Part B: Polym Phys 2000, 38, 2714.
3. Seo, J.; Han, H. Polym Degrad Stab 2002, 77, 477.
4. Seo, J.; Jeon, J.; Lee, C.; Park, S.; Han H. J Appl Polym Sci 2001, 79, 2121.
5. Han, H.; Seo, J.; Ree, M.; Pyo, S. M.; Gryte, C. C. Polymer 1998, 39, 2963.
6. Seo, J.; Han, H. J Polym Sci Part B: Polym Phys 2001, 39, 669.
7. Seo, J.; Cho, K. Y.; Han, H. Polym Degrad Stab 2001, 74, 133.
8. Han, H.; Gryte, C. C.; Ree, M. Polymer 1995, 36, 1663.
9. Huang, J.; Cranford, R. J.; Matsuura, T.; Roy, C. J Appl Polym Sci 2003, 87, 2306.
10. Huang, J.; Cranford, R. J.; Matsuura, T.; Roy, C. J Membr Sci 2003, 215, 129.
11. Alfrey, T., Jr.; Gurnee, E. F.; Lloyd, W. G. J Polym Sci Part C: Polym Symp 1966, 12, 249.

12. Wu, J. C.; Peppas, N. A. J Polym Sci Part B: Polym Phys 1993, 31, 1503.
13. Liu, H.; Li, J.; Hu, Y. Fluid Phase Equilib 1999, 158–160, 1035.
14. Zeng, C.; Li, J.; Li, P.; Chen, T.; Chen, C. Polym Mater Sci Eng Preprints 2005, 93, 310.
15. Zhang, P.; Sun, B.; Xu, Y.; Chen, C.; Li, J. Polym Mater Sci Eng Preprints 2005, 93, 474.
16. Hu, G. Master's thesis, Tsinghua University, 2002.
17. Chen, C.; Han, B.; Li, J.; Shang, T.; Zou, J.; Jiang, W. J Membr Sci 2001, 187, 109.
18. Neogi, P.; Kim, M.; Yang, Y. AIChE J 1986, 32, 1146.
19. Li, Y.; Teng, T.; Lu, J.; Chen, G.; Li, J. Fluid Phase Equilib 1986, 30, 297.
20. Zhou, G.; Liu, X. Visioplasticity Theory; Publishing Institute of University of Science and Technology of China: Hefei, People's Republic of China, 1996.
21. Flory, J.; Rehner, P. J Chem Phys 1943, 11, 512.
22. Tong, J.; Gao, G.; Liu, Y. Thermodynamics of Chemical Engineering; Publishing Institute of Tsinghua University: Beijing, People's Republic of China, 1993; p 327.
23. Ma, P.; Zhao, X.; Li P.; Guo, J. Petrochem Technol 1994, 23, 593.
24. Masaro, L.; Zhu, X. X. Progr Polym Sci 1999, 24, 731.